High temperature behaviour of core materials used in GFRP composite sandwich panels

Pedro Pereira Lourenço

Instituto Superior Técnico

Abstract: Composite sandwich panels consisting of glass fibre reinforced polymer (GFRP) faces and rigid polymer foam cores are being increasingly used in civil engineering, such as in roofs, facades and floors of buildings, and in bridge decks, where they may be subject to elevated temperatures, due to the environmental exposure or fire action. Therefore, it is important to study the behaviour of their constituent materials at elevated temperatures. The present dissertation aims at studying the behaviour at elevated temperature of PUR and PIR rigid foams. To that end, an experimental and analytical study of the mechanical behaviour of those materials was developed using the diagonal tension shear (DTS), for a temperature range between 20°C and 150°C, analyzing the constitutive relation in shear, including the maximum shear stress (τ_{max}) and shear modulus (G). In addition, the fire reaction and the thermo-physical behaviour at high temperature of the foams was analyzed through cone calorimeter and DSC/TGA tests. The results showed the significant influence of elevated temperature on the mechanical properties in shear of both foams, with the PUR foam presenting better performance than the PIR foam. In the analytical study, the models developed allowed simulating the temperature dependence of the mechanical properties in shear of both foams, for the temperature range studied. In what concerns the fire reaction properties and the thermo-physical behaviour at elevated temperature, both foams showed similar behaviour, although the PUR foam produced more noxious gases.

Keywords: GFRP composite sandwich panels, polymeric foams, polyurethane (PUR), polyisocyanurate (PIR), elevated temperature, fire, shear behaviour.

1. Introduction

Currently, some of the most important challenges that civil engineering is facing are associated with the costs of maintenance and repair of structures built with traditional materials (in general, steel, reinforced concrete and wood), which have increased dramatically through recent years. In this context, there has been a growing demand for structural systems that use new materials that are more durable and require less maintenance during their life [1].

These comprise new lighter materials with high mechanical performance, less prone to degradation caused by aggressive environmental agents, and which require less maintenance over their service life. Among these new materials, fiber reinforced polymer (FRP) composites are currently assuming significant relevance [1] [2].

Sandwich panels composed by FRP composites are part of a wide range of applications of composite materials in civil engineering. These composite sandwich panels have been increasingly used in various industries, including the construction industry. This is due, in large part, to the advantageous characteristics of this structural system, including the high strength-to-weight and stiffness-to-weight ratios, the versatility of the materials that can be used, the possibility of integrating multiple functions into one element and the potential lower life cycle cost compared to traditional building materials. In addition, the relatively low weight of sandwich panels *versus* conventional structural materials (ex.: reinforced concrete, steel) further allows an overall reduction in weight to the remaining structural elements and foundations [3].

Sandwich panels typically consist of two rigid outer faces (in the context of the present dissertation, FRP composite face panels) and a reduced density core (ex.: polymer foams, balsa wood, honeycomb cores). In some production processes, a structural adhesive can be further used to promote the bond between the core and the faces [4].

The core materials that compose the sandwich panels may take several forms and typologies depending on the characteristics of the material or the functional and/or architectural requirements of the intended use. The main types of core materials typically used in sandwich panels are as follows: (i) corrugated cores; (ii) cores in honeycomb structure; and (iii) homogeneous cores.

For homogeneous cores, rigid polymer foams, metallic foams or natural materials, such as wood (often balsa wood) are typically used. The largest variety of homogeneous core materials is found in rigid polymer foams, using materials such as polyethylene terephthalate (PET), polyurethane (PUR), polyisocyanurate (PIR), polymethacrylimide (PMI) and polyvinyl chloride (PVC).

The materials comprising the cores of sandwich panels, namely rigid PUR and PIR polymer foams, are particularly susceptible to the action of elevated temperature due to the organic nature of their polymer matrix. The current legislation regarding this matter, requires that all materials used in construction comply with the requirements of the Building Products Regulation, so the reaction to fire (of the finished

product), which includes the spread of flames and production of toxic fumes and gases, must comply with this regulation [5].

Several authors have studied the mechanical behaviour at elevated temperature for a wide variety of polymer foams used as core materials in sandwich panels. The research carried out in the present study focuses particularly on rigid PUR and PIR foams, but due to the lack of information for these specific materials, other similar materials were also considered.

Benderly and Putter [4] studied sandwich panels comprising polymethacrylimide (PMI) foam cores, with a density of 205 kg/m^3. The panels were tested at three temperatures (ambient temperature not specified, -40 °C and 70 °C), under four-point bending. The aim of the authors was to characterize the PMI foam shear and compression behaviour. They observed reductions of 31% and 35% in shear and compressive strengths, respectively, between room temperature and 70 °C.

Grace *et al.* [6] also studied a PMI foam, with a density of 32 kg/m^3, subjected to compression tests at temperatures of -60 ºC, 22 ºC and 60 ºC, at different loading speeds. The authors reported a decrease in resistance with increasing temperature (particularly between -60 °C and 22 °C), an effect that was further reduced at higher loading speeds. In this study, the authors reported that the highest temperature at which the foam was subjected to was higher than its glass transition temperature (unspecified value), which had also occurred in the Benderly and Putter [4] study.

Garrido [3] studied the effect of temperature on the shear response of two polymer foams: PET foam with density of 94 kg/m^3 and PUR foam with density of 68 kg/m^3. According to the author, the glass transition temperature of the PET foam was 65 °C and 90 °C for the PUR one. While the service temperature range for PET foam can be easily exceeded in a variety of civil engineering exterior applications (ex.: bridge decks), the maximum service temperature of the PUR foam will be sufficient for most conditions encountered in service in civil engineering applications. The mass loss curve for the PUR foam, obtained from DMA analysis, showed two significant decreases, corresponding to peaks in the derivation of the mass loss curve, at temperatures of 274 ºC and 532 ºC. These peaks are directly related to two exothermic peaks in the heat flow curve, reflecting the decomposition process that the polymer material underwent. At these two instants of the decomposition process, the mass was reduced by approximately 45-50%. The decomposition temperatures, corresponding to the temperatures at which 5% of the sample mass is lost, were 241 °C for PUR foam and 326 °C for PET foam (35% higher than PUR foam). These temperatures are well beyond the maximum service temperature range for civil engineering applications of these materials.

Regarding the literature review presented above, one can conclude that there are still unanswered questions concerning the influence of elevated temperature on the mechanical behaviour of the constituent materials of the sandwich panels. The authors of the investigations carried out in this field have concluded that the mechanical properties of the material composition of the core, including the elasticity and shear moduli, suffer significant reductions when subjected to elevated temperatures (close to the glass transition temperature to show a direct influence on these properties).

The experimental campaign developed within the scope of this study intends to respond to part of the needs identified above, particularly with respect to the following aspects:

• Behaviour of rigid PUR and PIR foams under shear stresses, for a range of temperatures including the respective glass transition temperature. The developed campaign includes mechanical tests by the diagonal tension method (DTS), recently developed at IST.

• Comparative analysis of the behaviour of PUR and PIR rigid foams under fire and elevated temperature through DSC/TGA and cone calorimeter tests.

The experimental campaign presented is divided into three main parts: **(i)** the mechanical shear characterization at elevated temperature; **(ii)** the thermo-physical behaviour at elevated temperature; and **(iii)** the reaction to fire. The procedures and test methods used in the experimental campaign are presented, together with the presentation and discussion of the respective results.

The mechanical shear characterization aimed to assess the influence of temperature on the performance of those rigid foams, with the analysis of the following shear parameters: shear modulus (G) and maximum shear stress (τ_{max}). The tested temperatures ranged from ambient temperature up to 150 ºC, including the glass transition temperature (set at 90 ºC, according to [3]).

The behaviour of the rigid foams at elevated temperature aimed to assess the decomposition temperature (T_d). The cone calorimeter tests aimed at determining the reaction to fire behaviour, including the release of heat and the production of smoke and noxious gases to the atmosphere and the contribution to fire.

The final part of this paper comprises the modeling of the degradation of the shear properties with temperature, including the analysis of the accuracy of three different models suggested in the literature. Those models were suggested by the following authors: Gibson *et al.* [7], Correia *et al.* [8] and Mahieux *et al.* [9]. The shear parameters studied were the same analyzed in the experimental campaign, namely the shear modulus and the maximum shear stress.

2. Experimental campaign

2.1. Materials

The core materials used in the experimental campaign were two types of polymer foams: polyurethane (PUR) and polyisocyanurate (PIR) rigid foams. Both foams were supplied by the company *ALTO - Perfis Pultrudidos, Lda.*, with a nominal density of 40 kg/m^3, produced by the same two components: isocyanate (MDI) and polyol. The difference in their production is that the PIR foam is produced with an additional amount of MDI (relative to PUR); this component is currently known for its thermal stability.

The rigid PUR and PIR foams were supplied in blocks of the following dimensions: 1.2 × 0.4 × 0.13 m, as shown in **Fig. 1**. The bi-component resin chosen for the adhesive bond between the foam and the test pieces was identical the one used in [3] and was supplied by Sika - SikaForce 7710 L100 (component A) and SikaForce 7010 (component B). These two components, when combined, form a solid resin based on polyurethane, which ensures that the break in the DTS test is not through the interfaces, but through the fragile areas of the foam itself.

Fig. 1: Blocks of rigid PUR and PIR foams used at experimental campaign.

2.2. Shear tests at elevated temperature

After being exposed to elevated temperatures, the test selected for mechanical shear characterization of the foams was the diagonal tension shear (DTS) test. In order to assess the effect of temperature on the shear behaviour of these materials, it is necessary to perform tests for a wide range of temperatures (from room temperature to 150 °C), including the glass transition temperature of these materials, which allows to verify the consequences in the behaviour across the transition from the glassy state to the rubbery state.

The distribution of forces as well as the deformations imposed by this method are illustrated in **Fig. 2**. The force distribution and respective calculations are based on ASTM E519. The force acting on each face is given by $(\sqrt{2}/2)P$, which allows to calculate the shear stress (τ), through **Eq. (1)**,

$$\tau = \frac{\frac{\sqrt{2}}{2}P}{A} \quad \textbf{(1)}$$

where P is the applied force and A is the area of one face of the specimen in contact with the test pieces. The average contact area for the 4 faces of the specimen can be estimated by **Eq. (2)**,

$$A = \frac{(W+h)\times t}{2} \quad \textbf{(2)}$$

where *W* is the width of the test piece, *h* is the height of the test piece, and *t* is the thickness of the test piece. The distortion (γ) can be calculated by **Eq. (3)**,

$$\gamma = \frac{\Delta V + \Delta H}{g} \quad \textbf{(3)}$$

where ΔV is the vertical relative displacement, ΔH is the horizontal relative displacement and g is the diagonal length of the specimen, given by $(W+h)/2$. Finally, the shear modulus (G) can be calculated by **Eq. (4)**,

$$G = \frac{\tau_2 - \tau_1}{\gamma_2 - \gamma_1} \quad \textbf{(4)}$$

where τ_2 and τ_1 are values of shear stresses at two points of the linear elastic region of the shear-distortion stress curve and γ_2 and γ_1 are the respective distortions for these points.

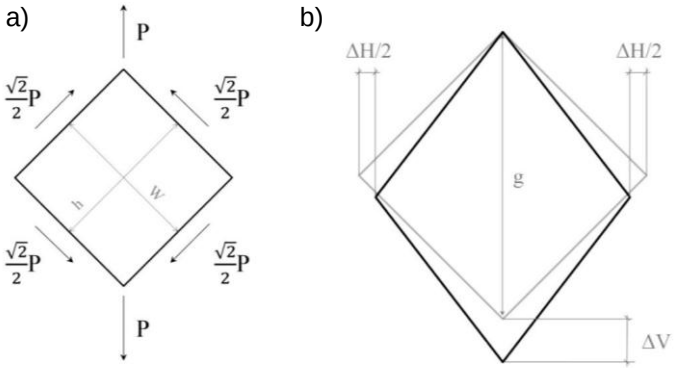

Fig. 2 - Calculation model for DTS test method: (a) force distribution, and (b) imposed deformation [3].

The deformations of the test pieces during the test were measured by the videoextensometry technique; for this purpose, target points were marked on one of their faces. The monitoring of the position of the target points throughout the test was carried out using a videoextensometer, which allows the identification of the targets in the test pieces and the subsequent comparison with their initial position, allowing to obtain shear stress-distortion curves. **Fig. 3** shows the geometry and dimensions of the specimen for the DTS test method.

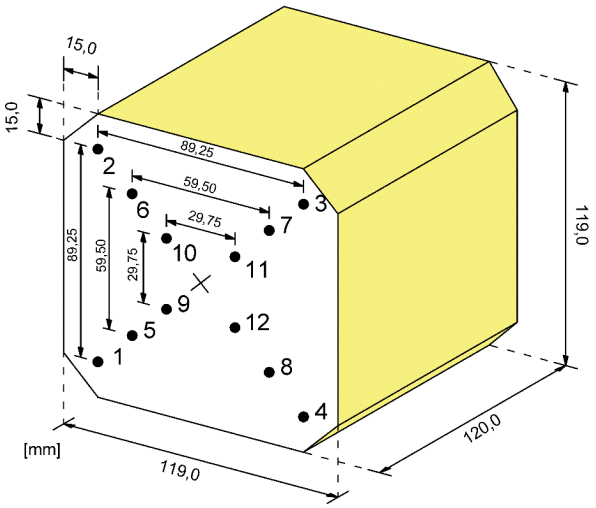

Fig. 3 - Geometry and dimensions of the test specimen for the DTS test method.

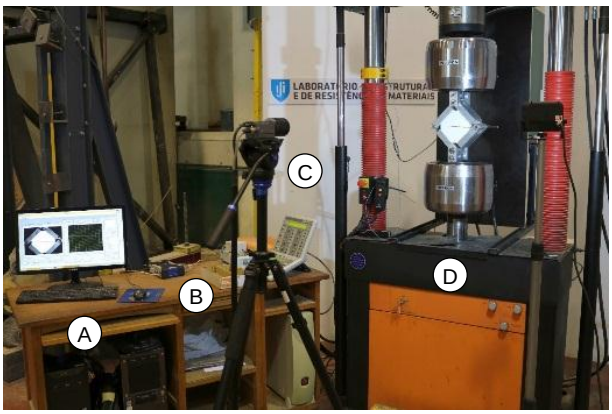

Fig. 4 - General view of equipment used at the DTS test: (A) monitoring computer, (B) data logger, (C) videoextensometer, and (D) *Instron*.

Fig. 4 shows the general view of the equipment used in the DTS tests at room temperature, including an *Instron* universal test machine (UTM), a videoextensometer, a data logger and a computer. The data loggers receive the signal transmitted by the load cell and defletometer of the UTS and the thermocouples. The computer allows the acquisition of data from the data logger and the videoextensometer through the *LabView* computer software, which interfaces the user, camcorder and controller of the *Instron* UMTM, allowing to register the applied load, the displacement of the machine and the positions of the points monitored. The *Instron* UTM used for the application of the load has a load capacity of 250 kN. Image capture was performed using a videoextensometer, consisting of a high definition Sony video camera. The heating of the test pieces was done through a *Tinius* Olsen thermal chamber, with internal dimensions of 605×205×205 mm.

In **Fig. 5 a)**, the main measurements of the DTS test mold, the depth of the metal rods and the height of the furnace are shown. **Fig. 5 b)** shows a test scheme (after rupture of a test specimen), where a dummy test piece was employed, connected to a thermocouple (**Fig. 6 a)**).

The temperature in the specimen was measured by a thermocouple of type K wire (with diameter of 0.25 mm), with the data being acquired by an HBM data logger, model MX 1609. The temperature inside the thermal chamber was also measured using a thermocouple, the results of which were compared with those measured at the center of the specimen. **Fig. 6 b)** shows the defletometer used for confirmation of displacements obtained by videoextensometry.

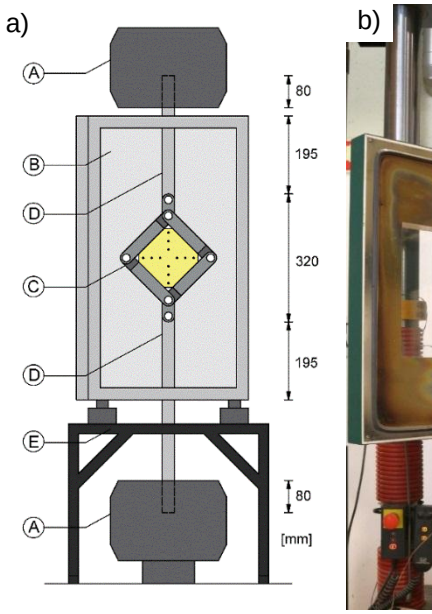

Fig. 5 - a) Representation of the test scheme: A) Instron gripper head, B) oven, C) test fittings, D) metal rod, E) oven support structure; and b) the actual test scheme.

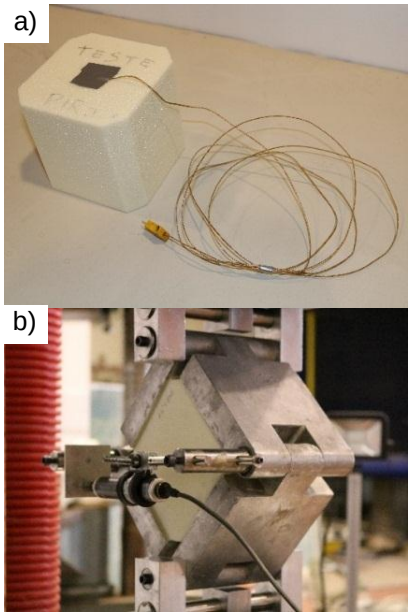

Fig. 6 - Auxiliary equipment to the DTS test: a) thermocouple with temperature control sample, and b) defletometer.

2.3. Thermo-physical behaviour at elevated temperature

In the present study, one of the focus of the experimental campaign is the characterization of rigid PUR and PIR foams when subjected to elevated temperatures. In this context, two evaluations were considered: the differential calorimetric analysis **(DSC)**, which allows to assess the temperature variation (ΔT) with associated heat fluxes; and the thermogravimetric analysis **(TGA)**, which allows recording the mass of the material tested during the imposed temperature variations, as well as the determination of the decomposition temperatures for each material. **Table 1** shows the summary of test specimens selected for the experimental program.

Table 1 - Summary of test specimens selected for the experimental program.

Material	Specimen	Atmosphere	Mass [mg]	Heating rate
PUR	PUR1	Air	2.239	5°C/min
	PUR2	Nitrogen	2.549	5°C/min
PIR	PIR1	Air	2.547	5°C/min
	PIR2	Nitrogen	2.549	5°C/min

The characterization of the two foams at elevated temperature was carried out in two types of atmosphere: the first one with nitrogen only, named pyrolysis of the material, without combustion due to the lack of oxygen; and the second one was an atmosphere of air, comprising oxygen, allowing the occurrence of combustion.

To perform the DSC/TGA analysis, it was necessary to use a thermal chamber that allows the recording of mass and heat flow, as well as the temperature of the specimen. The equipment used was a *Perkin* Elmer STA6000 machine. **Fig. 7** shows the holder chamber with crucible and the *Perkin* Elmer machine used at the experimental campaign.

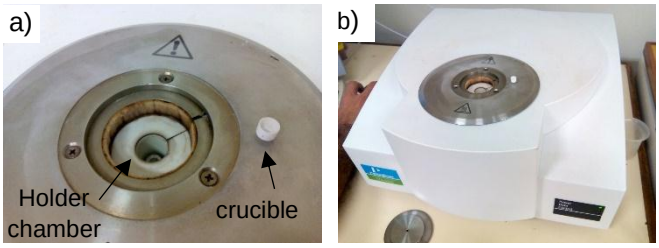

Fig. 7 – a) Holder chamber with crucible, and b) Perkin Elmer STA6000.

Fig. 8 presents the general view of the DSC/TGA test. The tests on each foam specimen were performed according to the following procedure:

1) Maintain the temperature at 30 °C for 5 minutes;
2) Heat from 30 °C to 800 °C at a rate of 5 °C/min;
3) Maintain the temperature at 800 ° C for 5 minutes;
4) Cool from 800 °C to 30 °C at a rate of 50 °C/min.

Fig. 8 - General view of the DSC/TGA test.

2.4. Reaction to fire

In order to assess the fire reaction of rigid PUR and PIR foams, it was decided to include in this dissertation a summary and an analysis of the main results of a study carried out by Proença *et al.* [10], using the **cone calorimeter** test method. The study evaluated the release of heat, smoke and toxic gases from the two foams, in order to assess and compare their fire reaction behaviour.

During the cone calorimeter test, several parameters were measured or calculated, of which the most relevant for the present study are: the heat release rate (HRR), the effective heat of combustion (EHC), the specific extinction area (SEA), the total heat released (THR), and the yield of CO_2 and CO.

The experimental program included the analysis of two specimens for each material (PUR and PIR). The specimens were tested with an area of 100x100 mm^2 and a height of 35 mm, as shown in **Table 2**.

Table 2 - Geometry and mass of the specimens tested by Proença *et al*. [8]

Specimen	Lx [mm]	Ly [mm]	t [mm]	Mass [g]
PUR 1	99.0	99.3	35.7	13.3
PUR 2	98.8	99.4	35.1	13.6
PIR 2	100.0	99.7	34.0	12.9
PIR 3	100.4	99.4	36.5	13.6

The authors carried out the tests on a *Stanton* Redcroft cone calorimeter, comprising the following elements: a sample holder, a conical heat source (conical electric radiator that emits a constant heat flux up to 100 kW/m^2), a load cell and an exhaust system. **Fig. 9** presents the *Stanton* Redcroft cone calorimeter testing machine, from both frontal and lateral views.

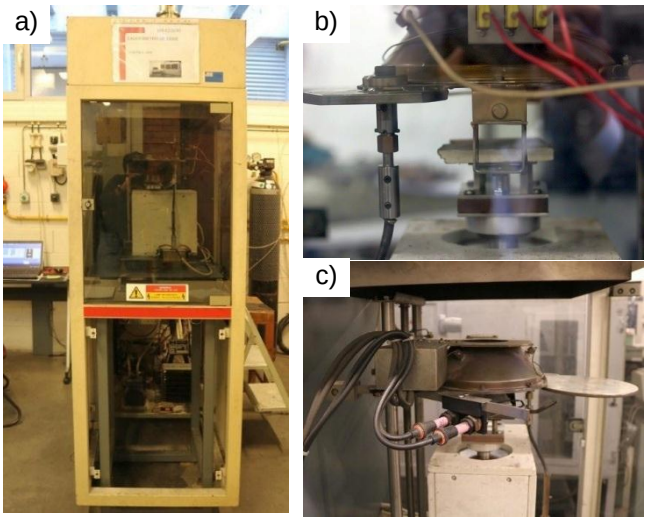

Fig. 9 – Stanton Redcroft cone calorimeter testing machine: a) front view, b) right lateral view, and c) left lateral view (adapted from [10])

3. Experimental results and discussion

3.1. Shear tests at elevated temperature

The DTS tests provided the shear stress *vs*. distortion curves, for both rigid foams of PUR and PIR, for the selected temperatures. It was also possible to capture images of the specimens using videoextensometry to illustrate the failure modes. The curves of shear stress vs. distortion, allow the assessment of two properties, which are essential to characterize the mechanical behaviour in shear, namely the shear modulus and the maximum shear stress.

Fig. 10 a) shows the influence of temperature on the constitutive relationship in shear for PUR foam. This figure shows that only the curves for the tests at room temperature (25 °C) reflect a linear behaviour, which is directly associated with the brittle rupture of the specimens tested at that temperature. A gradual reduction of shear stiffness is also clear for the tests carried out at higher temperatures (50, 80, 110 and 150 °C), with the largest reduction occurring at 80 °C, which can be explained by this temperature range including the glass transition temperature of the material. For the test carried out at 150 °C, a relatively small shear stress was obtained, only 25% of the maximum shear stress at room temperature.

Fig. 10 b) shows the shear stress vs. distortion curves, for the PIR foam using the DTS test method. As verified in the tests for the PUR foam, also for the PIR foam, brittle failure occurred only on tests carried out at room temperature, visible from the elastic-linear curve progress at this temperature. The gradual reduction of shear stiffness with increased temperature is also quite clear for the PIR foam. The tests conducted at the same temperature display similar curves, allowing to conclude that there have been no major discrepancies in the implementation of the test, reflecting a good representativeness of the sample.

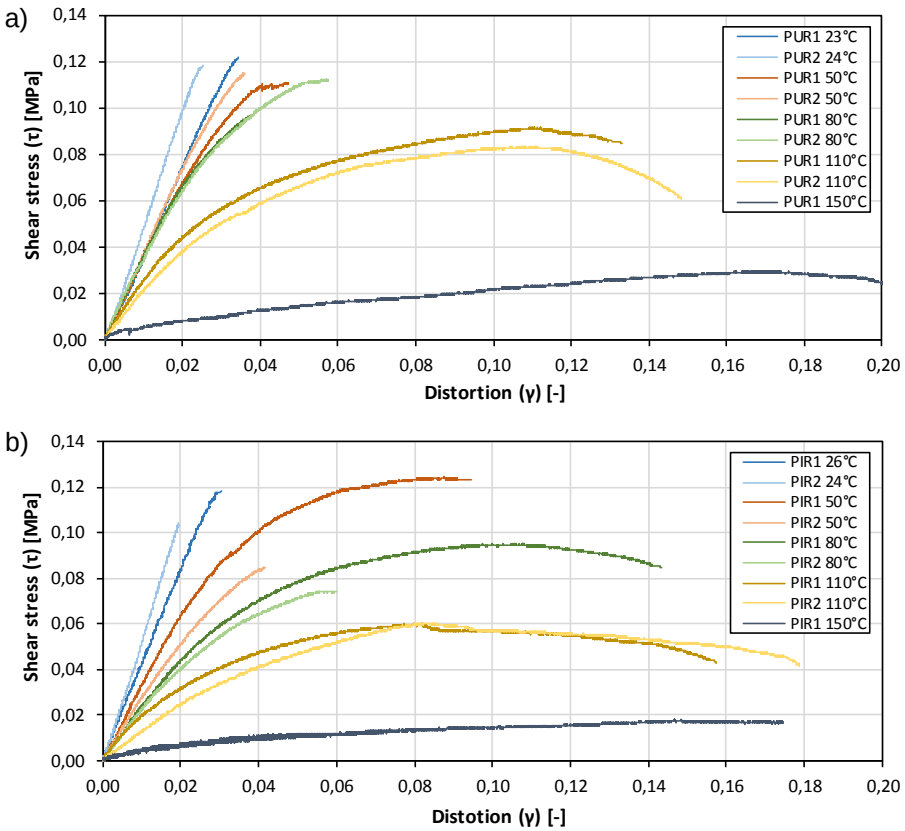

Fig. 10 – Shear stress vs. distortion curves on the outer square of the DTS test at different temperatures for: a) PUR foam, and b) PIR foam.

Table 3 shows the summary of the results obtained for the shear modulus and for the different temperatures studied, both for PUR and PIR foams, obtained through the DTS test method. The absolute and normalized values of the shear modulus at room temperature are presented.

Table 3 - Summary of DTS test results for the shear modulus of PUR and PIR foams.

PUR foam			PIR foam		
T [°C]	$G_{médio}$ [MPa]	$(G/G_{20})_{médio}$	T [°C]	$G_{médio}$ [MPa]	$(G/G_{20})_{médio}$
24	4.58	1.00	25	4.70	1.00
50	3.60	0.79	50	2.78	0.59
80	3.25	0.71	80	1.93	0.41
110	1.74	0.38	110	1.21	0.26
150	0.22	0.05	150	0.19	0.04

The room temperature is the only temperature in which PIR foam presented higher shear modulus, in comparison to the PUR foam. For all other temperature ranges, the shear modulus of the PUR foam is higher: 30% higher at 50 °C, 68% at 80 °C and 44% at 110 °C, with the biggest difference occurring at 80 °C. For PUR foam, the most significant reduction for shear modulus occurs at 110 °C, which is only 38% of the value obtained at room temperature, while for the PIR foam, the biggest reduction occurs right at 50 °C, being the shear modulus only 59% of the obtained at room temperature.

Table 4 presents the summary of the results obtained for the maximum shear stress, for absolute and normalized values at the different temperatures studied, for both PUR and PIR foams, obtained through the DTS test. The values of the maximum shear stress are relative to the room temperature, for which the maximum shear stress values were obtained, being very similar for both foams. It is possible to verify that the maximum shear stress is always higher in the PUR foam than in the PIR foam, with the exception of tests at 50 °C, when the averages were equal (0.11 MPa).

Table 4 - Summary of DTS test results for maximum shear stress of PUR and PIR foams.

PUR foam			PIR foam		
T [°C]	τ_{med} [MPa]	$(\tau/\tau_{20})_{med}$	T [°C]	τ_{med} [MPa]	$(\tau/\tau_{20})_{med}$
25	0.12	1.00	25	0.11	1.00
50	0.11	0.94	50	0.11	0.93
80	0.11	0.87	80	0.09	0.76
110	0.09	0.73	110	0.06	0.54
150	0.03	0.25	150	0.02	0.16

For PUR foam, the greater reduction at the shear stress occurred for the range 110-150 °C (reduction of 48%), with a fairly minor reduction (14%) for the range of 80-110 °C. In the case of PIR foam, the greater reduction for shear stress occurred in the range 110-150 °C (38%), but with significant reductions from the previous ranges, 17% at 50-80 °C and 22% at the range 80-110 °C. To conclude, these results show that the decrease at maximum shear stress occurred at lower temperatures in PIR foam than in PUR foam.

3.2. Thermo-physical behaviour at elevated temperature

The results obtained from the DCS/TGA analysis are curves relating the mass loss and heat flow, depending on the temperature. The curves on pyrolysis and combustion scenario are the main results that allow to assess differences in the behaviour at elevated temperature, for both rigid PUR and PIR foams.

The results obtained for pyrolysis scenario through the DSC/TGA test are represented in **Fig. 11**. It is evident the existence of temperature ranges where the progress is consistent and different for both foams, these being: 30-200 °C, 200-250 °C, 250-350 °C, 350-600 °C and 600-800 °C. The temperature of decomposition was determined as the temperature in which 50% reduction occurs in property values ($T_{d,m}$); in this case the percentage of mass loss. At pyrolysis, the temperature of decomposition for PUR foam was 312 °C, while for the PIR foam it was 292 °C. The value of the decomposition temperature for PIR foam has a relatively reduced value, being the progress in the percentage of mass loss more pronounced at the beginning of the range considered, compared with PUR foam.

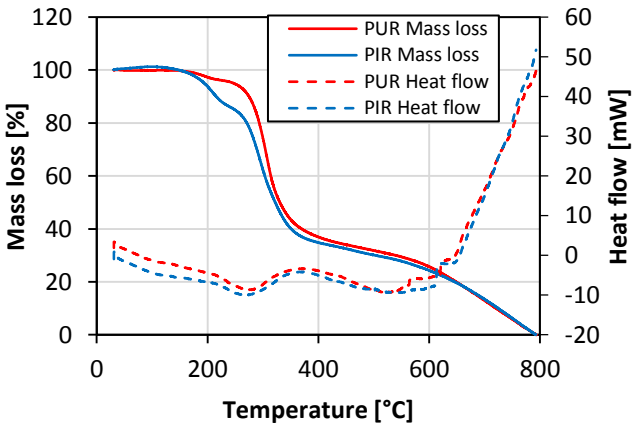

Fig. 11 - Results of the TGA test for the pyrolysis scenario in rigid PUR and PIR foams.

In pyrolysis, the PIR foam showed greater reductions in mass for relatively small temperatures (up to 250° C), as in this range 15% of lost mass, while the PUR foam lost only 6%. The largest reduction in the mass of the test occurred in the temperature range 250-350° C, which is related to the structural links breaks, representing a loss of 51% of mass and 45%, for PUR and PIR. **Table 5** presents the percentage of mass loss for pyrolysis atmosphere of rigid foams of PUR and PIR. In conclusion, for an atmosphere of nitrogen, PIR foam offers lower thermal resistance that PUR foam.

Table 5 - Percentage of mass loss for pyrolysis scenario of PUR and PIR foams.

Material	Mass loss				
	0°C to 200°C	200°C to 250°C	250°C to 350°C	350°C to 600°C	600°C to 800°C
PUR foam	3%	3%	51%	17%	26%
PIR foam	7%	8%	45%	16%	24%

The results obtained for the combustion through the DSC/TGA tests are represented in **Fig. 12**, to rigid foams of PUR and PIR. The decomposition temperature for PUR foam was 312 °C, while for the PIR foam was 285 °C. The decomposition temperature value for PIR foam, as in both combustion and pyrolysis scenarios, presented a relatively reduced value, due to the fact that the progress in the percentage of mass loss was more pronounced at the beginning of the range considered, compared with PUR foam.

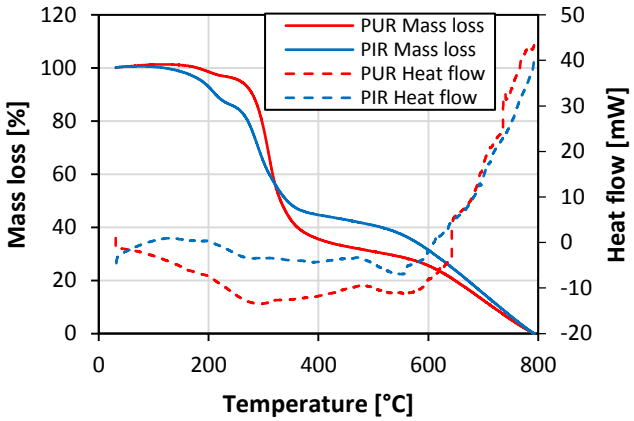

Fig. 12 - Results of the TGA test for the pyrolysis scenario in rigid PUR and PIR foams.

As occurred for the tests in an inert environment, PIR foam was more volatile than PUR foam at relatively low temperatures (up to 250 °C), losing 15% of its mass, while the PUR foam lost only 4%. The largest mass loss of the test occurred in the temperature range of 250-350 °C, having lost 53% of mass for PUR and 36% for PIR. **Table 6** presents the percentage of mass loss for oxygen atmosphere of rigid foams of PUR and PIR.

Table 6 - Percentage of mass loss for combustion scenario of PUR and PIR foams.

Material	Mass loss				
	0°C to 200°C	200°C to 250°C	250°C to 350°C	350°C to 600°C	600°C to 800°C
PUR foam	1%	3%	53%	18%	25%
PIR foam	7%	8%	36%	18%	31%

In conclusion, and regarding the behaviour of the rigid foams at elevated temperature, PUR foam has a slightly better behaviour than PIR foam, as for inert and oxidative atmospheres, being only outdated in terms of thermal resistance, from 320 °C in the combustion scenario. In any case, within the scope of the *EasyFloor* Project, it is concluded that any of the foams can be used, and there are no clear advantages at elevated temperature behaviour between the two rigid foams.

3.3. Reaction to fire

During the tests, both PUR and PIR foams showed almost instantaneous combustion, with average time to ignition of 7 s for PUR foam and 5 s to PIR foam. The foams burned intensely while producing large amounts of smoke. The flame extinction occurred, on average, after 4 min and 2 min, for PUR and PIR foam, respectively. **Fig. 13** summarizes the main reaction to fire properties, namely the HRR, EHC, SEA, CO2 and CO, to the average values of the test specimens of PUR and PIR (maximum values throughout the test according to the PUR foam). The PUR specimens showed worse performance on all properties, except on the production of CO, where both PIR specimens showed slightly worse performance. These results confirm the benefits of PIR foam over PUR foam, regarding the production of heat and smoke in a fire scenario.

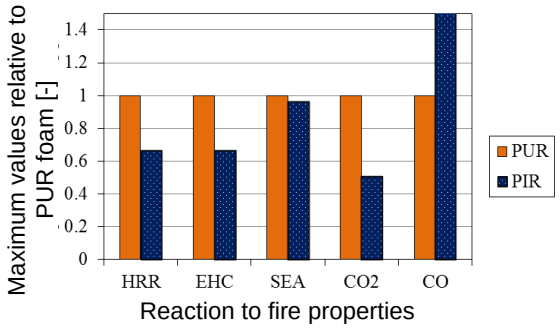

Fig. 13 – Maximum values for reaction to fire properties relative to PUR foam (adapted from [10]).

Table 7 presents the main expected results for the SBI test, in particular the respective fire growth rate (FIGRA) for each of the tested rigid core foams, and the reaction to fire class (Euroclass). Those estimates were calculated by Proença *et al.* [10] using the *Conetools* software.

Table 7 - Main properties on reaction to fire for the core materials of SBI test simulation (adapted from [10]).

Specimen	PUR 1	PUR 2	PIR 2	PIR 3
THR_{600S}	15.1	16.1	11.0	10.6
Max FIGRA [W/s]	2691.8	3908.4	2574.6	2735.9
Euroclass [-]	E or worse	E or worse	E or worse	E or worse

In fact, the rigid foam which showed better reaction to fire was the PIR foam; however, both were classified as Euroclass E or worse. These results prove the better thermal stability of PIR foam and the worst performance PUR foam, regarding the reaction to fire properties. The results obtained in this experimental campaign point the

essential need to include fire protection in the design of the *EasyFloor* sandwich panels.

4. Modelling of properties degradation with temperature

4.1. Description of models and parameter estimation

The properties of a material may or may not be significantly reduced, depending on the property in question, and in order to quantify this reduction, equations that could potentially fit the experimental results were fit. The three analytical models used in this study were originally developed for FRP materials, but since the foams are also from polymeric nature, it is expected to exhibit the same temperature relaxation process and fit the results of the present study. Three models of degradation chosen from literature for evaluation are presented, being these the models of Gibson *et al.* [7], Correia *et al.* [8] and Mahieux et al. [9].

In the model of Gibson *et al.* [7], the variation of a generic mechanical property P with temperature T, can be described by the following equation,

$$P(T) = P_u - \frac{P_u - P_r}{2} \times (1 + \tanh[k'(T - T_{g.mech})]) \quad \textbf{(5)}$$

where P_u is the property at ambient temperature and P_r is the property after glass transition (but before decomposition); $k'$and $T_{g.mech}$ are parameters obtained by fitting to the experimental data. According to Mahieux *et al.* [9], a mechanical property can be computed as a function of temperature through the following equation. based on Weibull distribution,

$$P(T) = P_r + (P_u - P_r) \times \exp[-(T/T_0)^m] \quad \textbf{(6)}$$

in which T_0 is the relaxation temperature and m is the Weibull exponent, both of them numerically fitted to the experimental data. More recently, Correia *et al.* [8] suggested the following model based on Gompertz statistical distribution shown in **Eq. (7):**

$$P(T) = (1 - e^{Be^{C \times T}}) \times (P_u - P_r) + P_r \quad \textbf{(7)}$$

where B and C are parameters obtained from fitting the modelling curve to the experimental data.

4.2. Results and discussion

The analytical modeling described in this section involved detailed mechanical shear behaviour characterization, for rigid foams of PUR and PIR, subjected to elevated temperatures, which has contributed to the benchmarking of models that express the degradation of mechanical properties as a function of temperature for core material in sandwich panels. **Table 8** shows the parameter estimation and EMPA for different models. **Fig. 14** and **Fig. 15** present the comparison between analytical modelling and experimental results for both parameters.

Table 8 – Simulation of shear mechanical properties for core foams – parameter estimation and absolute mean percentage error (AMPE) for different models.

Model	Parameter	PUR foam		PIR foam	
		τ_{max}	G	τ_{max}	G
Gibson *et al.* [7] Eq. (5)	k' [-]	0.028	0.021	0.024	0.020
	$T_{g.mech}$ [ºC]	115.5	94.5	102.2	69.1
	AMPE (%)	8.42	27.37	14.91	22.61
Correia *et al.* [8] Eq.(6)	B [-]	-37.605	-7.362	-14.736	-4.886
	C [-]	-0.035	-0.026	-0.031	-0.030
	AMPE (%)	11.34	40.69	18.05	25.93
Mahieux *et al.* [9] Eq. (7)	m [-]	16.088	11.355	13.233	9.295
	T_0 [-]	398.7	381.3	387.6	359.0
	AMPE (%)	6.39	16.16	11.39	17.57

After the comparison of the results obtained by the selected models, the main conclusions are summarized:

- The models studied have a relatively similar progress, being able to approach, in general, the progress of the experimental results as function of temperature, for both the shear modulus (G) the maximum shear stress (τ_{max});
- The model proposed by Mahieux *et al*. was the one that presented consistently better approximations to the test data.

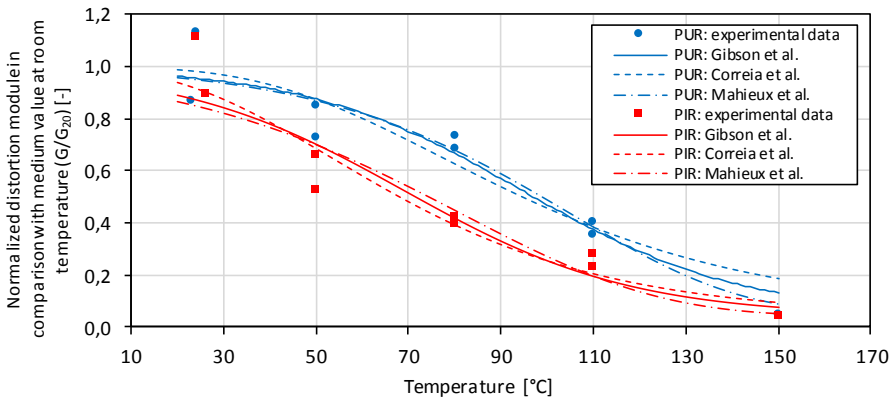

Fig. 14 – Comparison between the analytical modelling for normalized shear modulus and average value at room temperature (G/G_{20}), as a function of temperature.

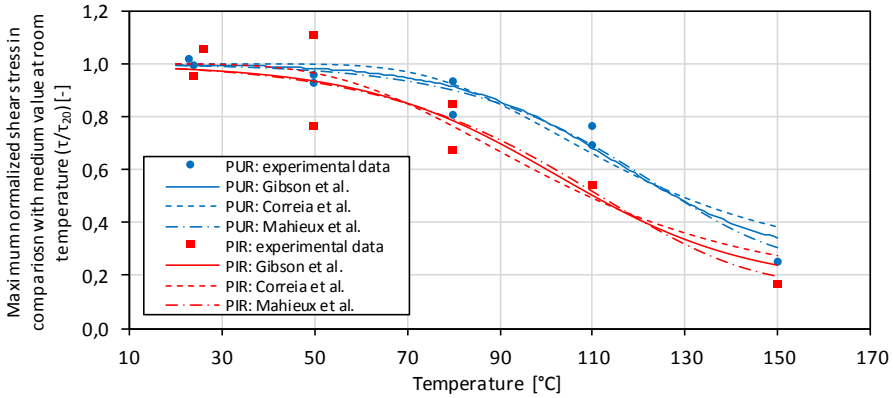

Fig. 15 – Comparison between the analytical modelling for normalized maximum shear stress and average value at room temperature (τ/τ_{20}), as a function of temperature.

5. Conclusions

The present experimental and analytical study aimed at **(i)** characterizing the variation of shear properties of PUR and PIR foams from room temperature up to 150 ºC; **(ii)** assessing the accuracy and reliability of a set of models, suggested in the literature, to predict the degradation with temperature of those properties, and **(iii)** analyze their thermo-physical behaviour at elevated temperature and reaction to fire. From the results obtained, the following main conclusions can be drawn:

1. For the shear modulus analysis, the values obtained for the PUR foam were superior to those obtained for PIR foam: 30% higher at 50 °C, 68% higher at 80 °C and 44% higher at 110 °C. The largest reduction in PUR foam occurred at the temperature range 80 °C-110 °C (38% of the modulus obtained at room temperature), while for the PIR foam such range was 50 °C-80 °C (59% of the modulus obtained at room temperature).

2. For the maximum shear stress analysis, for PUR foam, the biggest reduction occurred at the range 110-150 °C, with 48% reduction; and at the range 80-110 °C the reduction was only 14%. For PIR foam, the biggest reductions occurred at the range 110-150 °C, but with significantly smaller reductions than for PUR foam, 17% for 50-80 °C and 22% for 80-110 °C ranges.

3. Regarding the modelling of the properties degradation, the model that best described the results obtained in the experimental campaign, for the variation with temperature of both shear modulus and maximum shear stress, was the model of Mahieux *et al.*, with values of EMPA of approximately 16% and 7%, respectively.

4. In the DSC/TGA tests for air atmosphere, the decomposition temperature obtained was 312 °C and 285 °C, for the PUR and PIR foams respectively. The biggest reduction in the mass occurred at the temperature range 250-350 °C, with 53% of mass loss for the PUR foam and 36% for the PIR foam.

5. Regarding the reaction to fire, PUR specimens presented (predicted) FIGRA values, in general, higher than those obtained for the PIR specimens; however, both foams were classified as being Euroclass E or worse. PIR rigid foam presented better overall performance for the parameters of reaction to fire.

References

[1] J. R. Correia, “Fibre-Reinforced (FRP) Composites,” *Materials for Construction and Civil Engineering*, Springer International Publishing Switzerland, 2015.

[2] J. R. Correia, F. Branco, Características gerais dos compósitos FRP utilizados em aplicações da engenharia civil, Curso FUNDEC, Instituto Superior Técnico, 2016.

[3] M. Garrido, Composite sandwich panels floors for building rehabilitation, PhD Thesis, Instituto Superior Técnico, 2016.

[4] D. Benderly, S. Putter, “Characterization of the shear/compression failure envelope of Rohacell foam,” *Polymer Testing, Vol. 23*, Rapra Technology, Fevereiro 2004, p. 51–57.

[5] J. Correia, F. A. Branco, J. Ferreira, Y. Keller, T. Bai, “Fire protection systems for building floors made os pultruded GFRP profiles - Part 1: Experimental investigations,” *Composites Part B: Engineering*, 2010, pp. Vol. 41, N. 8, pp. 617-629.

[6] I. Grace, V. Pilichuk, R. Ibrahim, E. Ayorinde, “Temperature effect on nonstationary compressive loading response of polymethacrylimide solid foam,” *Composite Structures, Vol. 94*, 2012, pp. 3052-3063.

[7] A. Gibson, Y. Wu, J. Evans, “Laminate theory analysis of composites under load in fire,” *Journal of Composite Materials, Vol. 40*, 2006, pp. 639-658.

[8] J. Correia, M. Gomes, J. Pires, F. Branco, “Mechanical behaviour of pultruded glass fibre reinforced polymer composites at elevated temperature: experiments and model assessment,” *Composite Structures, Vol. 98*, 2013, pp. 303-313.

[9] C. Mahieux, K. Reifsnider, S. Case, “Property modelling across transition temperatures in PMC's: part 1. Tensile Properties,” *Applied Composite Materials, Vol. 8*, Netherlands, Kluwer Academic Publishers, 2001, pp. 217-234.

[10] M. Proença, M. Garrido, J. R. Correia, “Fire properties of the EASYFLOOR sandwich panels constituents,” Instituto Superior Técnico, Lisboa, 2017.